Robust Contactless Pulse Transit Time Estimation Based on Signal Quality Metric

Xijian Fan[a,*], Tardi Tjahjadi[b]

[a]*Nanjing Forestry University, Longpan Road, Nanjing 210037, CHINA*
[b]*University of Warwick, Gibbet Hills Road, Coventry CV4 7AL, UK*

ABSTRACT

The pulse transit time (PTT) can provide valuable insight into cardiovascular health, specifically regarding arterial stiffness and blood pressure. Traditionally, PTT is derived by calculating the time difference between two photoplethysmography (PPG) measurements, which require a set of body-worn sensors attached to the skin. Recently, remote photoplethysmography (rPPG) has been proposed as a contactless monitoring alternative. The main problem with rPPG based PTT estimation is that motion artifacts affect the shape of waveform leading to the shift or over-detected peaks, which decreases the accuracy of PTT. To overcome this problem, this paper presents a robust pulse-by-pulse PTT estimation framework using a signal quality metric. By exploiting the local temporal information and global periodic characteristics, the metric automatically assesses pulse quality of signal on a pulse-by-pulse basis, and calculates the probabilities of the pulse peak being the actual peak. Furthermore, in order to cope with over-detected and shift pulse peaks, Kalman filter complemented by the proposed signal quality metric is used to adaptively adjust the peaks based on the estimated probability. All the refined peaks are finally used for pulse-by-pulse PTT estimation. The experiment results are promising, suggesting that the proposed framework provides a robust and more accurate PTT estimation in real applications.

Keyword: Pulse transit time; Signal quality metric; Remote photoplethysmograpy; Physiological signal processing

1. Introduction

Pulse transit time (PTT) is the time for a pulse waveform to travel between two arterial sites. As a vital clinical indicator, the PTT has been used not only for estimating blood pressures continuously in Ma and Zhang (2005); Martin et al. (2016); Carek et al. (2017), but also for measuring arterial stiffness in Yoon et al. (2009). Depending on the equipment used and applications, PTT can be defined as various time intervals: 1) the time interval between the R-wave of the electrocardiogram (ECG) and the following pulse peak of the photopelthysmogram (PPG) as in Mukkamala et al. (2015); and 2) the time interval between PPG waveforms measured from two body parts as in Gesche et al. (2012). In this study, we use the PTT as the time interval between two pulse peaks of the PPG within the same cardiac cycle.

Recent studies have demonstrated the potential of contactless pulse measurement via a camera based on the same physiological principles as contact PPG (cPPG) using body-worn sensor. This contactless technique for pulse detection termed remote photo-

*Corresponding author
e-mail: xijian.fan@njfu.edu.cn (Xijian Fan)

plethysmography (rPPG), has been widely used for estimating various physiological parameters such as heart rate (HR), respiratory rate (RR) and heart rate variability (HRV), etc. However, to the best of our knowledge, only two studies in Jeong and Finkelstein (2016) and Shao et al. (2014) attempted to use contactless way to detect PTT. Jeong et al. use high speed camera to extract rPPG and estimate PTT in Jeong and Finkelstein (2016), using a hand holder to prevent motion. However, such setting could not be suitable in real life as free movement should be allowed in daily monitoring. Shao et al. in Shao et al. (2014) find PTT by estimating between two rPPGs from face and palm regions, and average the PTTs over a temporal window to improve the accuracy. PTT exhibits physiological variation along the time, which is also a useful indicator of cardiovascular state as in Ding et al. (2017). Averaging over a temporal window may fail to track the variation of PTT. Thus, to retain the variation, it is reasonable to estimate PTT pulse by pulse, not simply using temporal averaging.

Both of the aforementioned studies adopt the traditional PTT estimation method used in cPPG, which directly estimate PTT using the maximum peaks over each waveform pulse, and use the time interval of two detected peaks within the same cardiac pulse to define the PTT. However, these studies ignore the fact that the rPPG is relatively weak, and is prone to noise such as motion artifacts as it is acquired remotely. A weak signal makes the actual peak difficult to observe, while motion artifacts could distort the shape of certain rPPG pulses leading to the disappearance of peaks or unnecessary over-detected peaks. PTT estimation directly using the maximum peaks in such noisy rPPG yield unreliable results. Thus, it is important to determine whether each pulse peak is an actual peak or not (highly affected by motion artifacts), and only the actual peaks can be used for further PTT estimation.

To this end, we propose a robust framework for PTT estimation using the information of the signal quality. More specifically, we propose an effective signal quality metric for rPPG called RP_SQM which describes the signal strength and the degree of motion artifacts. This metric is capable of indicating the confidence the detected peaks are actual peaks and the reliability for PTT estimation. The metric is based on the fact that the quality of a rPPG signal can be described by signal strength and the degree of motion artifacts. The strength of rPPG signal varies along different skin regions due to vessel distribution under the skin, while the existence of motion artifacts could distort waveform morphologically. To realize pulse-by-pulse PTT estimation, we need to accurately detect every peak related to cardiac pulse as the PTT estimation candidates. Thus, we cannot simply discard those peaks with low confidence metric as some of them may relate to a normal cardiac pulse. To solve this problem, we adopt the Kalman filter (KF) to adjust the peaks, where the proposed metric is applied to automatically update the estimation of KF. By doing so, those pulse peaks with high confidence metric are enhanced, while those with low confidence metric are suppressed and adjusted by their neighboring peaks. PTT estimation are thus facilitated using the adjusted peaks. The framework of the PTT estimation is shown in Fig. 1.

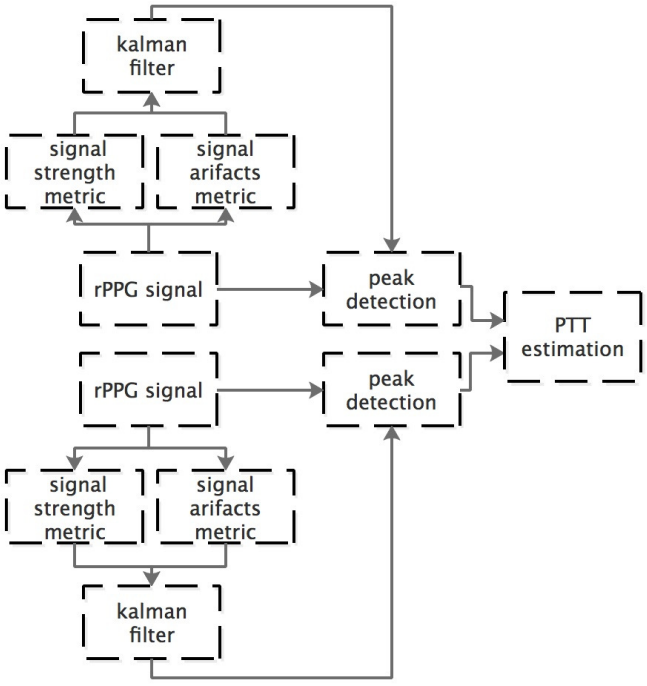

Fig. 1. The framework of the proposed method.

We summarize our main contributions as follows:

- We develop a self-scoring strategy using the proposed signal quality metric (RP_SQM) to identify the reliability of rPPG based on the global characteristics and local temporal information. To the best of our knowledge, it is the first attempt on the computation of signal quality metrics applied to rPPG signal.

- We adopt the proposed quality metric to automatically update Kalman Filter to detect the actual peak of rPPG, where the shift or over-detected peaks are eliminated to improve the PTT estimation.

The rest of paper is organized as follows. Section 2 presents the details of the propose method. Section 3 presents the experiments and evaluation results. Finally Section 4 concludes the paper.

2. Methodology

To measure PTT, two rPPG signals from two body parts are required. We select the face and palm regions as the region of interests (ROIs) for rPPG extraction due to the convenience of measurement and the relatively good signal quality as in Kumar et al. (2015).

The raw rPPG signal associates with the variation of blood volume due to the heart beat, where the light absorption variation caused by hemoglobin change in blood forms the periodic characteristics of rPPG. The amplitude of light absorption variation with

blood volume is very small compared with that of the average remittance, appearing as a small alternating current (AC) component added to a large direct current (DC) component. The optical signal of the rPPG can be represented as in Lam and Kuno (2015):

$$I_i(t) = \alpha_i \beta_i (S_0 + \gamma_i S_0 \text{Pulse}(t) + R_0), \tag{1}$$

where, Pulse(t) is the normalized ideal rPPG signal, S_0 is the average scattered light intensity from the ROI of the skin with white light illumination, R_0 is the diffuse reflection light intensity from the surface of the ROI of the skin, the subscript i denotes the color channel, α_i is the power of the ith color light, β_i is the power of the ith color light in the diffuse reflection spectrum of the skin, and γ_i is the AC/DC ratio of a rPPG in the ith color channel, which relates to the vessel distribution. The spectral characteristics of the environmental illumination and the skin remittance are both considered in this optical signal model of rPPG. Eq. 1 describes the rPPG operation in an ideal case. When the subject is moving, the motion will modulate all three optical rPPG signals in the RGB channels in the same way, as in

$$I_i(t) = \alpha_i \beta_i (S_0 + \gamma_i S_0 \text{Pulse}(t) + R_0) M(t), \tag{2}$$

where $M(t)$ is the motion modulation on the ideal rPPG.

In order to deal with motion, it is desirable to track the ROI to make the extraction of rPPG robust. However, the face is not rigid, which means the different regions within the ROI move separately especially during the appearance of expression. Thus, it is necessary to track different regions within the ROI independently. In our work, to improve the robustness, we divide the ROI into a number of local regions, and track these local regions to extract rPPG signal using de Haan and Jeanne's method as in De Haan and Jeanne (2013).

PTT estimation highly relies on the quality of rPPG, it is thus desirable to select high quality rPPG signals. To this end, the signal quality metric is proposed to assess the reliability of the extracted rPPG.

2.1. Signal Quality Metric for rPPG

The accuracy of PTT estimation depends on the quality of the rPPG. Two main factors can be used to describe the quality: signal strength and the degree of motion artifacts in rPPG. Based on these, we propose the signal quality metric to identify the good quality signal which is used for PTT estimation.

Signal Strength Metric. The strength of rPPG varies along different regions of skin surface as in Kumar et al. (2015). This is because the change of blood flow contributing to rPPG relies on the blood perfusion in the skin region, which in turn is determined by the distribution of vessels underneath the skin within the region. The skin region with less vessels (e.g., non-skin region such as eyes) results in limited blood perfusion, which contributes more noise and degrades the extracted rPPG signal. In order to obtain an

accurate PTT estimation, the signals with good strength are needed. Thus, it is desirable to automatically identify the good rPPG and select them for estimation.

A typical rPPG signal is quasi-periodic, and has a fundamental frequency of oscillation corresponding to heart (pulse) rate. Therefore, the spectral power of the typical rPPG signal is highly concentrated in a small frequency band around the pulse rate. A weak strength signal have more noise (e.g., limited blood perfusion), and such noise are random and not periodic leading to a more flat frequency distribution. Based on the spectral characteristics of the rPPG, we estimate the metric as a ratio of power of recorded near the pulse rate to the power of the noise, i.e.,

$$\text{SSM} = \sum 10\log_{10}\frac{\sum(\hat{S}(f)^2 U(f)}{\sum(\hat{S}(f)^2(1-U(f))}, \tag{3}$$

where $\hat{S}(f)$ is the spectrum of rPPG computed using Discrete Fourier transform (DFT) and $U(f)$ is a binary template window indicating whether frequency component f is attributed to the signal ($U(f) = 1$)) or to noise ($U(f) = 0$), i.e.,

$$U(f) = \begin{cases} 1 & \text{if } \|f - \text{HR}_{in}\| \leq \Delta f \\ 1 & \text{if } \|f - 2\text{HR}_{in}\| \leq 2\Delta f \\ 0 & \text{otherwise} \end{cases}, \tag{4}$$

where Δf denotes a small region in the frequency domain, and HR_{in} is the initial heart rate. SSM can be regarded as the signal-to-noise ratio. The denominator of Eq. (3) denotes the residual power of the spectrum within the heart range frequency [f-HR_{in}, f+HR_{in}], which can be regarded as the noise component of the signal. Since the signal always contains noise, the denominator of Eq. (3) is always non-zero. The second condition in Eq. 4 is due to the harmonic in the frequency domain. Specifically, when transformed to the frequency domain, the energy of the signal is often not only located near the fundamental frequency (i.e., f), but is also distributed near the multiple integers of the fundamental frequency (e.g., $2f$). Thus, the first harmonic $2f$ is also regarded as a wanted signal, and the second condition is used to extract the signal energy.

Motion Artifacts Metric. Even as tracking method tracks the different local regions within the ROI faithfully, motion artifacts still exist. This is because even very small motion of the subject relative to camera can lead to a change in the direction of incident light and reflected light. Such change in light direction affects the intensity of pixels, leading to the shape change of rPPG signal in a very short time period. The shape change could cause the drift or disappearance of peaks. We aim to capture the pulse with such motion induced peak change, and allocate less confidence to them. Here, we assume that the pulse rate related rPPG signal changes slowly, not showing sudden discontinuity. Thus, the distance of a peak associated with a pulse to its neighboring peaks is nearly constant. This distance is defined as inter peak interval (IPI), which is determined by initial heart rate HR_{in} as $\text{IPI} = 60/\text{HR}_{in}$. In our case, Fast Fourier transform (FFT) is applied to the extracted local rPPG signal to obtain an initial HR, where the initial HR is defined as the most dominant peak, considering only the spectral band between 40 and 240 bpm. Majority voting is used to select

the HR. Ideally, the successive IPI remains constant. However, motion artifacts cause the change of pulse shape, where the peak may shift from its actual location. Accordingly, the IPI between motion affected peak and its neighboring peaks will change, which is not well related to the initial heart rate. Thus, we define a Gaussian distribution to describe motion artifacts metric (MAM), i.e.,

$$\mathrm{MAM} = \sum_{k=1}^{2} \frac{\exp\left(-a * (D_k - \mathrm{IPI})^2\right.}{2}, \tag{5}$$

where a is the amplitude of the Gaussian distribution, k denotes the number of neighboring peaks, and D_k is the difference between a peak and its neighboring peaks. In an ideal case the difference between neighboring peaks have a distance of IPI; in case of a mis-detected peak, its neighboring peaks should not be the multiples of IPI. For a distance below or greater than 0.5*IPI, we assume that this neighboring peak is mis-detected or corresponds to another reference peak. The probability decreases with the distance of the neighbor peak from the center peak. We multiply SSM and MAM to form the final rPPG Signal Quality Metric referred as RP_SQM.

2.2. PTT Estimation Based on RP_SQM

By self-scoring the rPPG using the metric RP_SQM, the reliability of each pulse peak is determined. We need to adjust the peaks with low metric to estimate pulse-by-pulse PTT. To this end, KF is adopted to realize the automatic adjustment of peak location in our framework. This choice is motivated by KF's ability to track short-term stationary signal and real-time capability. In addition, KF enables an elegant inclusion of signal metric for more reliable estimation. The simplified KF algorithm used in our case is given by

$$x(n) = Ax(n-1) + \omega(n-1), \tag{6}$$

$$y(n) = Hx(n-1) + \nu(n-1), \tag{7}$$

where $x(n)$ is the state, $y(n)$ is current observation (raw inter-peak interval), $\omega(n)$ is the process noise, and $\nu(n)$ is the observational noise. A is the state parameter which controls the updating of state, and H is the observation parameter which controls the updating of observation. The two noise covariance matrices possess normal probability distributions $Q(n)$ and $R(n)$, i.e.,

$$\omega \sim N(0, Q(n)) \tag{8}$$

$$\nu \sim N(0, R(n)). \tag{9}$$

In addition to the proposed rPPG metrics, another novelty of this work is in applying the proposed metric into KF to weight inter peak interval estimation. As the Kalman weight is determined by Q and R, in order to integrate the metric information, we design

R to be time-varying and use the metric to update it. We set Q to be constant. Thus, the KF's time-varying observational noise covariance matrix is modeled as

$$R(n) = R \cdot (1 - \text{RP\_SQM}(n)). \tag{10}$$

This function tends to zero as the RP_SQM tends to unity. This allows the KF to use the current observation with confidence, and elevating the Kalman weight K. At low metric RP_SQM, R forces the KF to reduce K, and hence use the previous observation with more confidence. After KF filtering, all the peaks in rPPG are detected as PTT candidates, and PTT estimation are then computed.

3. Experiments and Results

To evaluate the performance of our proposed signal quality metric based method, we conducted two sets of experiments. We evaluated the performance in detecting the positions of pulse peaks and the accuracy in estimating PTTs comparing with the existing rPPG based PTT estimation methods using two qualitative measures: the mean absolute difference (MAD) and the normalized error rate in Gil et al. (2010) which is defined as:

$$\text{ER}_{no}(\%) = \frac{1}{N}\sum_{n=1}^{N}\frac{|I_{gt}(n) - I_{detected}(n)|}{|I_{gt}(n+1) - I_{gt}(n)|} \times 100, \tag{11}$$

where I_{gt} and $I_{detected}$ are respectively pulse peaks (or PTTs) manually annotated by three experts in the data and automatically detected by the algorithms. In the experiment, three experts who have strong background in medical and signal processing were selected for the annotation of the ground truth signal. The strategy of manual annotation is based on the following principles: 1) the difference values between two adjacent peaks range from 15ms to 80ms; 2) if there are multiple candidate peaks, the expert could make the decision based on the shape of the related peaks, which can eliminate the distortion of sudden motion; and 3) the peaks are selected based on the three experts' observations using majority voting. Furthermore, two statistical measures: sensitivity and precision are also employed to assess the usefulness of the proposed method in practice, where sensitivity is a measure of the ability of the proposed method to eliminate unsuitable peaks in accordance with the manual elimination, while precision is a measure of the ability of the proposed method to keep suitable peak in accordance with the manual selection. The sensitivity and precision are defined as:

$$\text{Sensitivity} = \frac{\text{TP}}{\text{TP} + \text{FN}} \tag{12}$$

$$\text{Precision} = \frac{\text{TP}}{\text{TP} + \text{FP}}, \tag{13}$$

where TP denotes true detected peaks, FN denotes false mis-detected peaks, and FP denotes false detected peaks.

3.1. Peak Detection Evaluation

To evaluate the performance of the proposed peak detection method, we used MAHNOB-HCI in Soleymani et al. (2012) and Vicar datasets in Tasli et al. (2014). The MAHNOB-HCI database consists of RGB sequences of 784x592 video frames recorded at 61 frames per second (fps) of human subjects exhibiting facial emotions in response to visual stimuli (from a computer monitor). In addition to video footage, the subjects' ECG readings were also recorded at 256 Hz with synchronized timings to the videos provided. Some sample images from a subject sequence in MAHNOB-HCI dataset are shown in Fig. 2.

Fig. 2. Sample images from MAHNOB-HCI dataset.

In the Vicar dataset, the ground truth cPPG is provided and synced with the captured video. Ten subjects with age ranging from 20 to 35 were used. The 720x1280 video sequences were recorded at 30 fps, and each has an average duration of 90 seconds. A CMS-50 Pulse Oximeter attached to the subject's fingertip was used to generate the ground truth pulse signal (i.e., cPPG). Due to the data licence agreement, we cannot present sample signals here.

In the experiments, we detected the peaks in aligned ground truth signal (ECG in MAHNOB and PPG in Vicar) as ground truth peak location. Then, we extracted rPPG signal from video, and implemented the maximum peak based algorithm which is used in rPPG based PTT estimation as in Jeong and Finkelstein (2016); Shao et al. (2014) for comparison. To further illustrate the advantage of our method, we also used other two conventional peak detection algorithm (the knowledge based rules in Jang et al. (2014) and the adaptive threshold method in Shin et al. (2009)) for comparison. These two methods are used for peak detection in motion existing cPPG, and rPPG also affected by motion. Thus, we used them for comparison. We use the aforementioned measures to evaluate the performance. The results on the MAHNOB-HCI in Soleymani et al. (2012) and Vicar datasets are shown in Table 1 and 2, respectively. The results indicate that the proposed method using signal quality metric outperforms the other

Table 1. Comparative evaluation of the proposed peak detection using MAHNOB

Measures	ER_{no}	MAD	Sensitivity	Precision
Maximum peak	0.50	8.27	**97.54**	98.12
Knowledge based **in** Jang et al. (2014)	1.75	7.82	96.32	97.68
Adaptive threshold **in** Shin et al. (2009)	3.58	9.62	94.62	95.32
Proposed	**0.23**	**3.13**	97.35	**98.25**

Table 2. Comparative evaluation of the proposed peak detection using Vicar

Measures	ER_{no}	MAD	Sensitivity	Precision
Maximum peak	0.59	3.57	96.32	**97.25**
Knowledge based **in** Jang et al. (2014)	1.87	5.37	92.51	93.34
Adaptive threshold **in** Shin et al. (2009)	4.04	6.81	94.05	95.24
Proposed	**0.20**	**1.43**	**97.83**	97.02

peak detection methods. This is because the proposed method employs the temporal information and automatically optimizes the peak location based on the signal pulse quality. Furthermore, the two peak detection methods used in cPPG show a relatively low performance in our rPPG case. This is because these methods identify the surrounding of actual pulse peaks due to the large shape variation in rPPG. Tables 1 and 2 respectively show the proposed method performs worse than the method of maximum peak in sensitivity and precision. This is because the proposed method mis-detects true peaks in some cases.

3.2. PTT Evaluation

Since there is no publicly available dataset for contactless PTT estimation, we created a dataset, VideoPTT, in our laboratory to validate the PTT estimation. Six healthy subjects were tested in the experiments with age varying from 25 to 32. This age range was selected as it is similar to that used in MAHNOB-HCI, which generally includes subjects with good health conditions and these subjects are available in our laboratory. An RGB camera on a tripod stand (to stabilise the image capture) was used to record 640x480 video sequences which include the face and palm regions recorded at 120 fps for rPPG extraction. The ground truth PTT is determined by the manually annotated peaks from two acquired rPPGs. To make the comparison fairly, we implemented the existing rPPG based PTT estimation method (referred as Baseline) in Jeong and Finkelstein (2016); Shao et al. (2014) and the proposed method using the same strategy, which computes the mean PTT over a 10s window. The measures including Mean absolute difference (MAD), standard deviation (SD) of difference and root mean squared error (RMSE) between ground truth and the methods are shown in Table 3. MAD is a measure of the bias of PTT estimates, while RMSE and SD are measures of error variability of PTT estimates. Furthermore, to illustrate the pulse-by-pulse performance of the proposed PTT estimation, we used sliding window to obtain pulse-by-pulse PTT, and used the measures of ER_{no} for evaluation, which is also shown in Table 3.

Table 3. Comparative evaluation of the proposed PTT estimation using VideoPTT

Measures	MAD	SD	RMSE	ER_{no}
Baseline **in** Shao et al. (2014)	6.43	5.15	10.31	0.72
Proposed	**5.49**	**4.38**	**8.84**	**0.58**

From Table 3, we can see that the proposed method using signal quality metric outperforms the existing rPPG based PTT method directly using peak in terms of both pulse-by-pulse basis and average over a time window. The contaminated pulse peaks could be identified, and automatically adjusted by the proposed method. Thus, the proposed method is robust to motion artifacts, and is suitable for real applications.

In our experiments, signal quality metric automatically identifies the bad signal segments, where the peaks are regarded as false peaks and are thus removed. This increases the accuracy of the peak detection. Signal metric based Kalman filter automatically refines the peak location and increases the accuracy of detected peaks, and thus PTT.

The study in Mukkamala et al. (2015) concludes that wave reflection impacts the shape of blood pressure waveforms, but its interference is small at the minima of the waveforms. Thus, it is important to validate the rPPG signal, e.g., that maximum peaks are not significantly distorted before applying the proposed method. This is to ensure that the efficacy of the proposed method. However, validating the signal is beyond the scope of this paper, and is left for a future work.

4. Conclusion

This paper presents the first attempt for automatic quality assessment of rPPG signal. We developed different algorithms, based on the specific characteristics of rPPG, to identify artifacts and compute the overall quality of rPPG. Moreover, the proposed metrics are applied to update Kalman filter to improve the peak location by highlighting the strong and clear pulse. The proposed method has been shown to be the preferred choice due to its robustness to morphological artifacts and its effectiveness in extracting PTT on a pulse-by-pulse basis. Future work will include generating larger database (e.g., including other age groups) for testing and improving the robustness of rPPG acquisition for better PTT estimation.

References

Carek, A.M., Conant, J., Joshi, A., Kang, H., Inan, O.T., 2017. Seismowatch: wearable cuffless blood pressure monitoring using pulse transit time. Proceedings of the ACM on interactive, mobile, wearable and ubiquitous technologies 1, 40.

De Haan, G., Jeanne, V., 2013. Robust pulse rate from chrominance-based rppg. IEEE Transactions on Biomedical Engineering 60, 2878–2886.

Ding, X., Yan, B.P., Zhang, Y.T., Liu, J., Zhao, N., Tsang, H.K., 2017. Pulse transit time based continuous cuffless blood pressure estimation: A new extension and a comprehensive evaluation. Scientific reports 7, 11554.

Gesche, H., Grosskurth, D., Küchler, G., Patzak, A., 2012. Continuous blood pressure measurement by using the pulse transit time: comparison to a cuff-based method. European journal of applied physiology 112, 309–315.

Gil, E., Bailón, R., Vergara, J.M., Laguna, P., 2010. Ptt variability for discrimination of sleep apnea related decreases in the amplitude fluctuations of ppg signal in children. IEEE Transactions on Biomedical Engineering 57, 1079–1088.

Jang, D.G., Farooq, U., Park, S.H., Hahn, M., 2014. A robust method for pulse peak determination in a digital volume pulse waveform with a wandering baseline. IEEE transactions on biomedical circuits and systems 8, 729–737.

Jeong, I.C., Finkelstein, J., 2016. Introducing contactless blood pressure assessment using a high speed video camera. Journal of medical systems 40, 77.

Kumar, M., Veeraraghavan, A., Sabharwal, A., 2015. Distanceppg: Robust non-contact vital signs monitoring using a camera. Biomedical optics express 6, 1565–1588.

Lam, A., Kuno, Y., 2015. Robust heart rate measurement from video using select random patches, in: Proceedings of the IEEE International Conference on Computer Vision, pp. 3640–3648.

Ma, T., Zhang, Y.T., 2005. A correlation study on the variabilities in pulse transit time, blood pressure, and heart rate recorded simultaneously from healthy subjects., in: International Conference of the Engineering in Medicine and Biology Society, p. 996.

Martin, S.L.O., Carek, A.M., Kim, C.S., Ashouri, H., Inan, O.T., Hahn, J.O., Mukkamala, R., 2016. Weighing scale-based pulse transit time is a superior marker of blood pressure than conventional pulse arrival time. Scientific reports 6, 39273.

Mukkamala, R., Hahn, J.O., Inan, O.T., Mestha, L.K., Kim, C.S., Töreyin, H., Kyal, S., 2015. Toward ubiquitous blood pressure monitoring via pulse transit time: theory and practice. IEEE Transactions on Biomedical Engineering 62, 1879–1901.

Shao, D., Yang, Y., Liu, C., Tsow, F., Yu, H., Tao, N., 2014. Noncontact monitoring breathing pattern, exhalation flow rate and pulse transit time. IEEE Transactions on Biomedical Engineering 61, 2760–2767.

Shin, H.S., Lee, C., Lee, M., 2009. Adaptive threshold method for the peak detection of photoplethysmographic waveform. Computers in biology and medicine 39, 1145–1152.

Soleymani, M., Lichtenauer, J., Pun, T., Pantic, M., 2012. A multimodal database for affect recognition and implicit tagging. IEEE Transactions on Affective Computing 3, 42–55.

Tasli, H.E., Gudi, A., den Uyl, M., 2014. Remote ppg based vital sign measurement using adaptive facial regions, in: Image Processing (ICIP), 2014 IEEE International Conference on, IEEE. pp. 1410–1414.

Yoon, Y., Cho, J.H., Yoon, G., 2009. Non-constrained Blood Pressure Monitoring Using ECG and PPG for Personal Healthcare. Plenum Press.